

Ages, distributions, and origins of upland coastal dune sheets in Oregon, USA

Curt D. Peterson^{a,*}, Errol Stock^b, David M. Price^c, Roger Hart^d,
Frank Reckendorf^e, Jon M. Erlandson^f, Steve W. Hostetler^g

^a *Portland State University, Portland, Oregon 97207–0751, USA*

^b *Griffith University, Brisbane, Queensland, 4111, Australia*

^c *Wollongong University, Wollongong, New South Wales 2522, Australia*

^d *Department of Oregon Geology and Mineral Industries, Newport, Oregon 97365, USA*

^e *Reckendorf and Associates, 950 Market. St. NE, Salem, Oregon 97301, USA*

^f *University of Oregon, Eugene, Oregon 97403, USA*

^g *US Geological Survey, Oregon State University, Corvallis, Oregon 97331, USA*

Received 17 June 2006; received in revised form 22 January 2007; accepted 1 February 2007

Available online 14 February 2007

Abstract

A total of ten upland dune sheets, totaling 245 km in combined length, have been investigated for their origin(s) along the Oregon coast (500 km in length). The ages of dune emplacement range from 0.1 to 103 ka based on radiocarbon (36 samples) and luminescence (46 samples) dating techniques. The majority of the emplacement dates fall into two periods of late-Pleistocene age (11–103 ka) and mid–late-Holocene age (0.1–8 ka) that correspond to marine low-stand and marine high-stand conditions, respectively. The distribution of both the late-Pleistocene dune sheets (516 km² total surface area) and the late-Holocene dune sheets (184 km²) are concentrated (90% of total surface area) along a 100 km coastal reach of the south-central Oregon coast. This coastal reach lies directly landward of a major bight (Heceta–Perpetua–Stonewall Banks) on the continental shelf, at depths of 30–200 m below present mean sea level (MSL). The banks served to trap northward littoral drift during most of the late-Pleistocene conditions of lowered sea level (–50±20 m MSL). The emerged inner-shelf permitted cross-shelf, eolian sand transport (10–50 km distance) by onshore winds. The depocenter sand deposits were reworked by the Holocene marine transgression and carried landward by asymmetric wave transport during early- to mid-Holocene time. The earliest dated onset of Holocene dune accretion occurred at 8 ka in the central Oregon coast. A northward migration of Northeast Pacific storm tracks to the latitude of the shelf depocenter (Stonewall, Perpetua, Heceta Banks) in Holocene time resulted in eastward wave transport from the offshore depocenter. The complex interplay of coastal morphology, paleosea-level, and paleoclimate yielded the observed peak distribution of beach and dune sand observed along the south-central Oregon coast.

© 2007 Elsevier B.V. All rights reserved.

Keywords: Coast; Dunes; Beaches; Oregon; Paleosea-level; Paleoclimate

* Corresponding author.

E-mail addresses: petersonc@pdx.edu (C.D. Peterson),
E.Stock@ens.gu.edu.au (E. Stock), dprice@uow.edu.au (D.M. Price),
roger_hart01@mac.com (R. Hart), frecken@open.org (F. Reckendorf),
jerland@darkwing.uoregon.edu (J.M. Erlandson),
steve@coas.oregonstate.edu (S.W. Hostetler).

1. Introduction

Although the upland coastal dunes of Oregon represent unique habitat, cultural sites, and recreational resources (Bannan, 1989; USFS, 1994; Shultz, 1998;

Erlandson et al., 1998) their origins have not previously been explained. The largest dune fields (40–60 km in length) are located on the south-central Oregon coast (Fig. 1). No large, upland dune fields are found in adjacent coastal regions of Washington, or northern California (Cooper, 1958, 1967). Unlike the lowland dune ridges that flank the Columbia River mouth (Rankin, 1983; Woxell, 1998; Reckendorf et al., 2001) the upland dunes of Oregon are not directly associated

with large river systems. Distinctive heavy minerals in Oregon coastal deposits trace the sand origins to rivers in southern Oregon and northernmost California (Schiedegger et al., 1971; Clemens and Komar, 1988). The northernmost California river sand was apparently transported north on the continental shelf during pre-Holocene periods of fluctuating sea levels.

Cooper (1967) mapped groupings of coastal dune fields in central and southern California (Fig. 1). Very

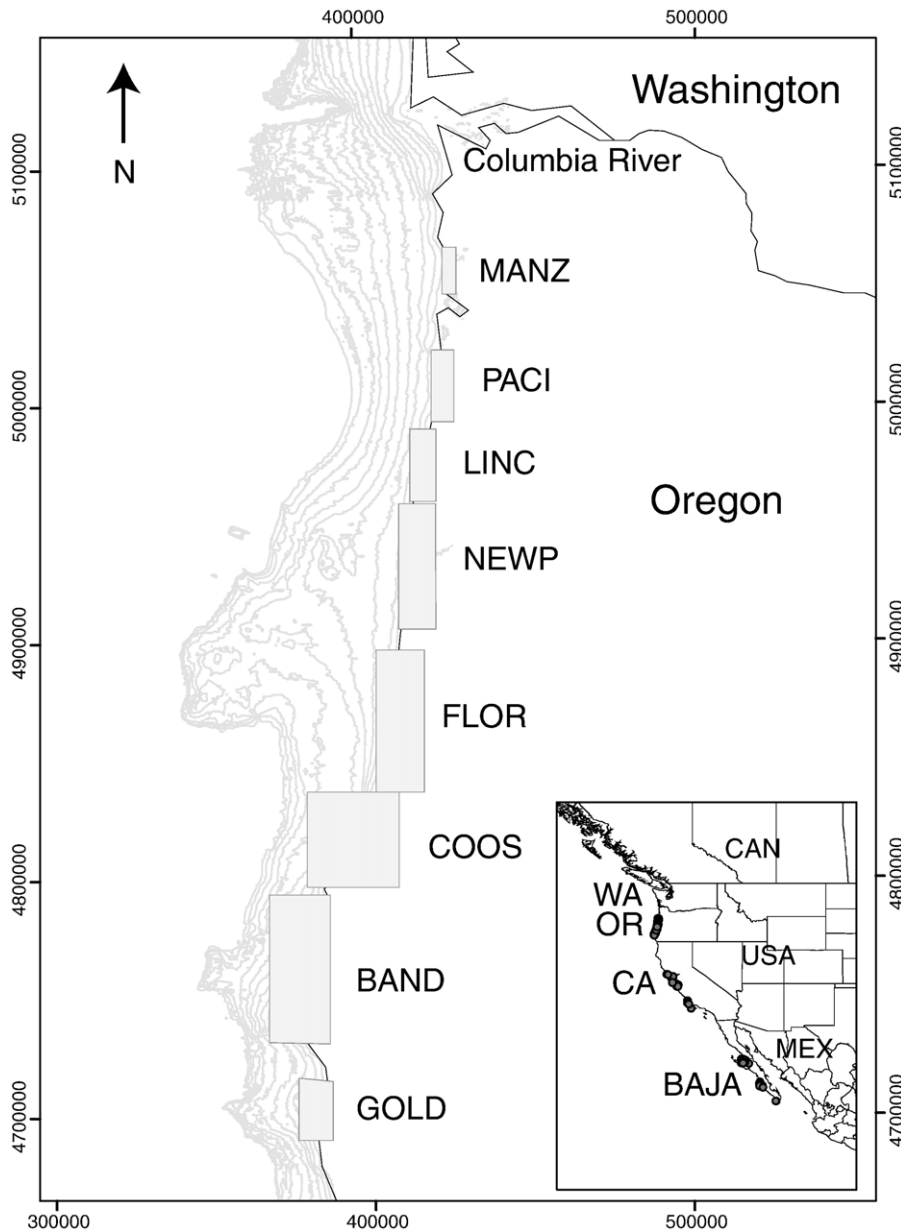


Fig. 1. Inset map (lower right) of major, upland, coastal dune fields (solid dots) in Oregon, California, and Baja California. The enlarged map of Oregon shows upland, dune-sheet localities (boxes) that are named (abbreviations) after prominent coastal cities. Map coordinates are in UTM Easting and Northings at 100 km intervals. Offshore bathymetry is shown in 20 m isobaths.

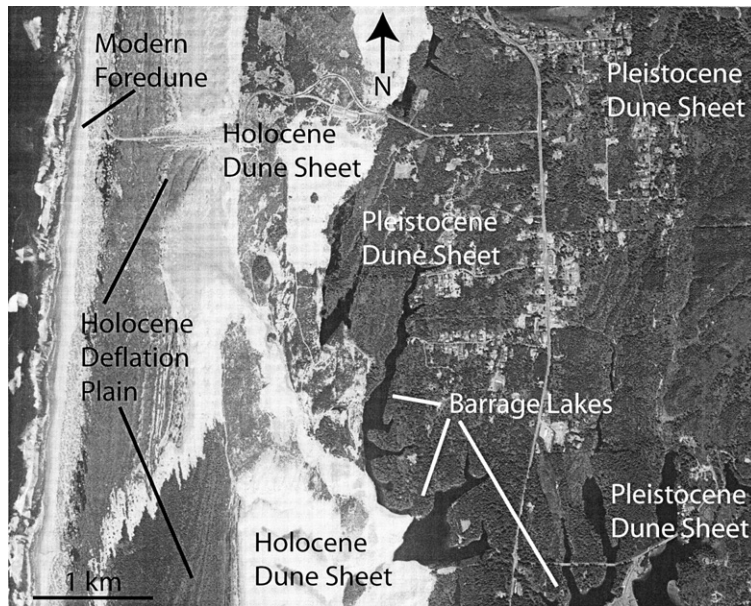


Fig. 2. Aerial infrared (gray scale) photograph of dunes and coastal development, located just south of Florence, Oregon (see FLOR dune sheet in Fig. 1). Active transverse and parabolic dunes (white shade) have migrated landward, abandoning foredunes and deflation-plain wetlands (darker shade) along the beach (figure left). The Holocene dunes have invaded forested terrain (darker shade) that developed on the Pleistocene dune sheet. The Pleistocene dune sheet and underlying marine terrace are dissected by coastal streams. Barrage lakes (black shade) fill tributary valleys that are now blocked by the Holocene dune sheet. Geohydrologic and geotechnical properties of the coastal plain soils are controlled by the dune-sheet deposits.

large fields of coastal dunes (50 km in width) are also present in the southern half of the Baja California peninsula (Murillo De Nava et al., 1999). These anomalous clusters of coastal dune fields are separated by long stretches of coastline (200–500 km) without significant dune cover. The largest, coastal dune fields in California are associated with pre-Holocene dune deposits (Bonilla, 1971; Dupre, 1975; Orme, 1992). The largest dune fields in Oregon are also associated with pre-Holocene dune deposits that mantle the uplifted coastal terraces (Cooper, 1958; Reckendorf, 1998). An understanding of the origins of the upland dunes in Oregon might shed light on the geomorphic development of other coastal dune complexes in the central west coast of North America, and in other continental coastlines.

In this paper we compile available radiocarbon (^{14}C) dates and present new thermoluminescence (TL) dates from the upland dune deposits of Oregon. The extensive dating control permits the discrimination of Holocene and Pleistocene emplacement ages for the dune deposits. Anomalous thick paleosols also separate these two periods of coastal dune sand supply and deposition (Peterson et al., 2006). Distributions of the contiguous dune deposits, i.e., dune sheets, are compared to former sea-level, paleoclimate conditions, and offshore topography. Emerging relations from these comparisons indicate that the upland dunes in Oregon originated from a sand depocenter that

was located on the emerged inner-continental shelf during low-stand conditions, and was reworked by waves during the Holocene marine transgression.

2. Background and field methods

Cooper (1958, 1967) mapped ‘recently-active’ coastal dunes, e.g., latest-Holocene dunes, in a pioneering effort that extended along the length of the US West Coast. Active remnants of the late-Holocene dunes are still evident on modern aerial photos and satellite images of the south-central Oregon coast (Fig. 2). Open dune habitat has significantly diminished during the last half century due to vegetative stabilization efforts (Carlson et al., 1991). Older dunes, e.g., pre-Holocene in age, mantle much of the central Oregon coastal plain (Reckendorf, 1975). They are currently obscured by forest cover, mass-wasting, and stream dissection. The pre-Holocene dune deposits in Oregon are not discriminated from underlying, but unrelated, shoreface deposits in published geologic maps (Schlicker et al., 1973; Schlicker and Deacon, 1974; Beaulieu and Hughes, 1975, 1976). The regressive shoreface deposits, typically 1–5 m thick, were deposited following marine high stands at ~ 80 , ~ 105 , and ~ 120 ka (Muhs et al., 1990). The Pleistocene dune sheets that overlie the regressive shoreface deposits are generally tens of thousands of years younger than the youngest marine

terrace (Peterson et al., 2006). In the field the Pleistocene dune sheets are differentiated from the regressive beach sands by their interbedding with paleosols, truncated root casts, peat horizons, and loess layers. These terrestrial interbeds reflect the episodic, subaerial deposition of the upland dune sheets. Groundwater alteration has variably cemented the oldest dune deposits (Grathoff et al., 2003), leading to their misidentification as sandstone bedrock or regolith in some geotechnical reports.

In order to establish the extent of stabilized dune deposits a field program was undertaken to map the landward pinchouts, or backedges, of the contiguous dune sheets. Interior sites within the dune sheets were profiled for stratigraphy, geotechnical properties, and groundwater redox conditions (Peterson et al., 2006). Four hundred sites were examined in roadcuts, sea cliffs, and auger holes of the upland dune deposits in Oregon. In this paper we compare the groundtruthed dune deposits to corresponding maps of marine terrace units.

Radiocarbon (^{14}C) dates from the upland dune deposits are compiled largely from archaeological reports. The cultural site ^{14}C dates typically post-date the emplacement ages of the hosting dunes. In this paper we present representative ^{14}C dates from cultural sites and other published sources with the stratigraphic context of the dated dune intervals. Preliminary radiocarbon dating of some pre-Holocene dune deposits proved their ages to extend beyond the reach of commercial ^{14}C dating, i.e., 40,000–45,000 radiocarbon years before present (^{14}C yr BP).

Luminescence dating is a well-established dating method for dune deposits that potentially extends the range of dating well beyond that of ^{14}C dating. (Aitken, 1985, 1998). Both optically-stimulated luminescence (OSL) and thermoluminescence (TL) dating techniques have been tested on upland dune deposits in Oregon where they yielded dates from 0.4 to 70 ka (Wiedemann, 1990; Heikkinen, 1994; Jungner et al., 2001; Beckstrand, 2001). For this study 38 sites were sampled for TL dating. The TL dating constrains the emplacement ages of the pre-Holocene dune sheets, and it establishes the rate of topsoil development in the Oregon dunes. The sample TL dating was conducted by David Price, at Wollongong University, Wollongong, Australia. Field techniques and supporting laboratory data for the TL dates are provided in Peterson et al. (2006).

The emplacement ages for the upland dune sheets are established on the bases of ^{14}C and TL dating, and on relative dating methods calibrated by the ^{14}C and TL dating techniques. The relative dating methods include the use of relative topsoil development and loess-enriched paleosols (Peterson et al., 2006). The loess-enriched paleosols are

present throughout the Pleistocene dune sheets but occur only as basal units in the Holocene dune sections.

3. Results

3.1. Upland dune sheets

The upland coastal dunes in Oregon are grouped into ten dune sheets, which are named after their corresponding coastal cities or prominent geographic features (Table 1). The dune sheets are separated by 1) rocky coastlines, 2) marine terraces lacking dune cover, and/or 3) tidal basin inlets. The boundaries between the central coast dune sheets, e.g., between Newport (NEWP) and Bandon (BAND), are somewhat arbitrary, as these dune sheets were probably contiguous on the inner-continental shelf during lower sea levels (Peterson et al., 2002).

The upland dune sheets range from one to 58 km in length, and from one to seven km in width. The longest dune sheets, NEWP, FLOR, COOS, BAND, are also the widest (Table 1). The two middle dune sheets, FLOR and COOS, are associated with the widest beaches, backshore and foredunes, e.g., active beaches, reaching at least 500 m in width, within the study area (Peterson et al., 1991; Fig. 2). Whereas the largest dune fields are clustered in the south-central Oregon coast the smallest dune fields occur at the extreme ends of the study area (Fig. 1). The northernmost and southernmost dune fields are separated from each other by three to ten km of narrow beaches and marine terraces without dune cover. The clustering of the upland dune fields within the 380 km-long study area of Oregon suggests a common sand source. However, the variations in size and spatial continuity of the dune sheets reflect different periods and mechanisms of dune sand supply.

Table 1
Upland dune sheets in Oregon

Dune-sheet location	Dune-sheet name	North end UTM-N	South end UTM-N	Maximum length N–S (km)	Maximum width E–W (km)
Manzanita	MANZ	5,064,360	5,060,400	4	1
Netarts	NETA	5,034,130	5,030,300	4	1
PacificCity	PACI	5,019,880	5,006,990	13	2
LincolnCity	LINC	4,983,930	4,960,490	23	1
Newport	NEWP	4,955,400	4,906,560	49	3
Florence	FLOR	4,893,000	4,844,400	45	6
CoosBay	COOS	4,834,890	4,800,020	35	7
Bandon	BAND	4,790,980	4,733,130	58	7
GoldBeach	GOLD	4,711,750	4,698,760	13	1
Crook Point	CROO	4,679,500	4,678,710	1	1

UTM coordinates are in meters north (N) and east (E) of section 10N, WGS1983.

Table 2
Dune-sheet radiocarbon ages

Sheet sample	UTM Northing	UTM Easting	Position material	$^{14}\text{C} \pm 1\sigma$ Lab calRCYBP	ID (Ref)
<i>MANZ</i>					
TI-57	5,060,900	428,250	(DT) char.	550–650	B40650(a)
<i>NETA</i>					
NETA	5,033,180	424,760	(DRT) char	1780–1920	B178109(b)
Park:a	5,022,850	423,900	(DRT) char	795–993	B124459(c)
<i>PACI</i>					
SLKa	5,017,100	424,650	(DT)	1418–1530	–(d)
SIKb	5,017,000	424,600	(DRB)	5489–5593	–(d)
CapeK1	5,007,790	423,490	W-(DT) char	0–286	B89157(b)
CapeK4a	5,007,790	423,490	W(DP) char	3630–3832	B89159(b)
CapeK8	5,007,790	423,490	W-(D) char	5302–5578	B89163(b)
<i>LINC</i>					
LINK16	4,978,760	420,100	E-(DP) wood	>40,000	–(b)
BB45a	4,964,300	415,950	(DRT) shell	4885–5297	B6332(e)
<i>NEWP</i>					
YH62a	4,947,400	414,650	(DRT) char	4523–4807	B3749(a)
YH62c	4,947,400	414,650	(DRB) char	5993–6267	B37500(a)
NEWP106	4,926,060	413,880	(DRB) char	3018–3152	B172772(b)
NEWP122	4,921,610	414,500	(DP) wood	>46,690	B148091(b)
NEWP86	4,933,080	414,770	(DRB) char	3600–3720	B148094(b)
LNC14b	4,927,150	413,900	(DRT) char	410–510	WSU1643(f)
NEWP151	4,906,560	411,960	(DRT) char	580–640	B172771(b)
NEWP152	4,888,720	410,460	(DRB) char	6460–6650	B148092(b)
<i>FLOR</i>					
LillyLake	4,882,600	410,700	(DL) wood	3084–3344	B67454(g)
FLOR12	4,872,750	409,950	W-(DB)wood	7668–7822	B84373(h)
LN-25a	4,868,510	410,440	(DT) char	450–630	B70385(i)
LN-25b	4,868,510	410,440	(DP) char	4410–4570	B70388(i)
FLOR36	4,862,100	410,080	(DT) char	563–697	B89164(h)
FLOR35	4,862,150	409,400	(DT) char	>46,500	B84374(h)
DO-130	4,850,000	407,800	(DL) char	3170–3390	–(j)
FLOR54	4,844,560	407,070	(DT) char	>45,300	B172773(b)
<i>COOS</i>					
CS-114a	4,815,500	399,000	E-(DT) char	2565–2935	B35551(k)
CS-114b	4,815,500	399,000	E-(DL) char	2990–3210	B70377(k)
CS-114c	4,815,500	399,000	E-(DP) char	3165–3345	B50018(k)
<i>BAND</i>					
BAND8	4,784,790	386,850	(DRB) char	1530–1780	B163484(b)
BAND9	4,784,640	386,810	W-(DT) char	35,400–36,200	B163485(b)
CS-136a	4,774,400	383,600	W-(DT) char	900–1080	B82085(l)
<i>GOLD</i>					
GOLD208a	4,702,210	382,800	(DRT) char	3950–4090	B172770(b)
GOLD208b	4,702,210	382,800	(DRP) char	5925–5975	B172774(b)
<i>CROO</i>					
CU31	4679700	384200	(DT) shell	540–720	B66879(m)
<i>Indian Sands</i>					
35CU675ab	4,668,000	387,300	(DT) char	28,500–29,160	–(n)

3.2. Dune-sheet ages

Calibrated radiocarbon dates (cal yr BP) from 36 representative sites in the upland dunes are compiled from archaeological reports and other sources (Table 2). The dated samples are identified with respect to their seaward position (W) or landward position (E) in the dune sheet, and to their stratigraphic position, including dune top (DT), dune base (DB) or internal dune paleosol (DP). The dune top ^{14}C dates are assumed to largely post-date dune emplacement. The dune top dates range from ~ 140 to $>46,500$ ^{14}C yr BP. The dune base and internal paleosol dates represent periods of dune field advance and deposition. These dates range from ~ 1620 to $>46,690$ ^{14}C yr BP. A total of six basal Holocene dates vary from 3018 to 7822 cal yr BP ($\pm 1\sigma$ error), and average about 5500 ^{14}C yr BP. The Holocene basal dates represent the onset of Holocene dune emplacement in the dated sites.

A total of 46 luminescence dates, including 38 new thermoluminescence (TL) dates, are compiled for the upland Oregon dunes (Table 3). The dune TL dates range from 0.4 to 103 ka. The oldest TL dates are relatively evenly distributed among the larger dune sheets, including PACI (84.8 ± 6.1 ka), LINC (73.3 ± 4.5 ka), NEWP (103 ± 7 ka), FLOR (70.1 ± 3.0 ka), COOS ($>65.5 \pm 4.1$ ka), and BAND (67.3 ± 21.7 ka). Basal dune dates at some sea cliff sites post-date the oldest inland dune deposits. In the NEWP dune sheet, a sea cliff basal deposit (NEWP93) and an inland dune site (NEWP94) have dates of 62.6 ± 4.1 and 103 ± 7 ka, respectively. The younger basal dates at the seaward dune sections reflect periods of marine truncation and/or deflation that locally eroded the oldest, seawardmost dune deposits.

Dune top dates generally increase in age from Holocene in the ‘seaward’ sites (0–7 ka) to Pleistocene in the ‘backedge’ sites (>20 ka) in the FLOR, COOS, and BAND dune sheets (Tables 2 and 3). Surface dune deposits are generally of Pleistocene age across the NEWP and LINC dune sheets. The dune deposits are

uniformly of Holocene age in the MANZ and CROO dune fields, located near the terminal ends of the study area. These newly established patterns of dune emplacement age are important to understanding the origins of the dune sheets, as discussed later in this paper.

3.3. Dune-sheet mapping

Vertical profiling of 400 sites in the Oregon marine terraces has permitted the discrimination of dune sheets from regressive shoreface deposits, colluvium, and bedrock regolith (Peterson et al., 2006). The groundtruthed dune sites are shown together with previously mapped marine terrace deposits in the four largest dune sheets, including NEWP, FLOR, COOS and BAND (Fig. 3A–D). The period of emplacement, either Pleistocene or Holocene, is designated for the surface dune deposit at each dune site.

The NEWP and BAND dune sheets are both dominated by Pleistocene dune deposits (Fig. 3A,D). The Holocene dunes constitute only narrow fringes along the coastline of the NEWP and BAND dune sheets. In comparison, Holocene dunes overlie most of the Pleistocene dune deposits in the FLOR and COOS dune sheets (Fig. 3B,C). Where the Holocene dunes are widespread, such as the FLOR and COOS dune sheets, the Quaternary Sand unit (qs) generally represents the extent of dune cover on the marine terraces. However, the undifferentiated marine terrace units fail to identify the extent of the Pleistocene dune deposits in any of the dune sheets. As shown by the regional dune dating (Tables 2 and 3) most of the Pleistocene dunes were emplaced ten’s of thousands years after the youngest, uplifted Pleistocene terrace was abandoned at 80 ka (Beckstrand, 2001). The Pleistocene dune sheets are entirely unrelated to the regressive beach deposits that mantle the terraces.

In order to evaluate the landward extent of the dune-sheet deposits we have identified representative dune backedge sites in each of the ten dune sheets. The surface

Notes to Table 2

UTM coordinates are in meters of section 10N, WGS1983.

Stratigraphic positions of the dated samples are denoted relative to 1) the western W- or eastern E- boundaries of the existing dune sheet, and 2) the Holocene or Pleistocene dune sequence including dune top (DT), internal dune paleosol (DP), or dune base (DB). Samples are also dated from dune ramps at Holocene sea cliffs (DR), dune barrage lakes (DL) which post-date the onset of dune-sheet emplacement, and Pleistocene shoreface deposits (S) which pre-date the emplacement of overlying dune sheets.

Material: charcoal/charred = char, wood/roots = wood, reservoir-corrected marine shell = shell.

Radiocarbon dates are calibrated using CALIB4.0 Stuiver et al. (1998).

The calibrated age includes the two endpoints that represent the range of age at 1-sigma (σ) uncertainty.

References: a = Minor (1991), b = Peterson et al. (2006), c = Minor (2006) d = Wiedemann (1990), (e) = Tasa and Connolly (1995), f = Clark (1991), g = Briggs (1994), h = Beckstrand (2000), i = Minor et al. (2000), j = Minor and Toepel (1986), k = Musil (1998), l = Tveskov et al. (1996), m = Moss and Erlandson (1995), n = Davis et al. (2004) and Davis (2006).

Table 3
Dune-sheet thermoluminescence ages

Sheet Site	UTM Northing	UTM Easting	Position TL/OSL	Age $\pm 1\sigma$ (ka)	Lab ID (Ref)
<i>NETA</i>					
NETA4	5,033,240	425,100	E-(DB) TL	6.5 \pm 0.5	W3488(a)
<i>PACI</i>					
SandLkLimb	5,017,100	424,650	(DT) TL	1.6 \pm 0.2	–(b)
SandLkCliff	5,017,000	424,600	W(DP) TL	11.2 \pm 1.5	–(b)
PACI18	5,015,418	425,449	E(DB) TL	84.8 \pm 6.1	W3388(a)
CapeK#1	5,007,800	423,500	W(DT) OSL	0.36 \pm 0.1	–(c)
CapeK#4	5,007,800	423,500	W(DP) OSL	4.29 \pm 1.08	–(c)
CapeKBase	5,007,800	423,500	W(DB) OSL	7.2 \pm 2.00	–(c)
<i>LINC</i>					
LINC6	4,981,325	421,400	E(DT) TL	>55.7 \pm 3.7	W3491(a)
LINC14	4,979,090	419,530	W(DB) TL	73.3 \pm 4.5	W3389(a)
<i>NEWP</i>					
NEWP5	4,955,040	417,640	E(DT) TL	>37.9 \pm 3.9	W3123(a)
NEWP22	4,951,540	417,620	E(DT) TL	>77.4 \pm 5.4	W3492(a)
NEWP44	4,944,420	416,920	E(DT) TL	50.5 \pm 4.7	W3592(a)
NEWP82	4,934,630	414,940	W(DRB) TL	4.1 \pm 0.4	W3493(a)
NEWP93	4,929,650	414,260	W(DB) TL	62.6 \pm 4.1	W3390(a)
NEWP94	4,929,640	416,550	E(DP) TL	103 \pm 7	W3124(a)
NEWP103a	4,926,910	413,830	W(DT) TL	46.4 \pm 4.1	W3392(a)
NEWP103b	4,926,910	413,830	W(S) TL	111 \pm 23	W3393(a)
NEWP137	4,914,090	413,790	E(DT) TL	60.5 \pm 5.4	W3586(a)
<i>FLOR</i>					
FLOR6	4,877,280	414,120	E(DT) TL	70.1 \pm 3.0	W2776(a)
FLOR11	4,872,800	409,950	W(DB) TL	7.3 \pm 0.6	W3115(a)
FLOR12	4,872,750	409,950	W(DT) TL	24.6 \pm 3.1	W2329(a)
FLOR13	4,872,550	413,090	E(DT) TL	6.4 \pm 0.7	W3114(a)
FLOR28b	4,864,850	413,990	E(DT) TL	37.2 \pm 4.8	W2328(a)
FLOR41	4,860,800	407,750	W(DT) TL	2.9 \pm 0.3	W2773(a)
FLOR40	4,860,910	408,420	W(DT) TL	1.5 \pm 0.3	W2774(a)
FLOR34	4,862,200	409,430	(DT) TL	32.4 \pm 8.2	W2331(a)
FLOR56	4,844,150	406,080	(DT) TL	45.3 \pm 3.1	W3116(a)
<i>COOS</i>					
COOS1	4,834,890	403,880	E(DT) TL	30.6 \pm 5.4	W3117(a)
COOS6	4,830,210	404,370	E(DT) TL	4.7 \pm 0.4	W2327(a)
COOS5	4,831,310	402,900	(DT) TL	5.6 \pm 1.6	W3118(a)
COOS12	4,825,870	403,690	E(DT) TL	3.9 \pm 0.4	W3119(a)
TenMileCKa	4,825,000	402,000	(DT) TL	1.06 \pm 0.1	–(d)
TenMileCKb	4,825,000	402,000	(DT) TL	18.3 \pm 1.5	–(d)
COOS17	4,820,420	402,720	E(DT) TL	32.9 \pm 3.6	W2775(a)
COOS20	4,819,270	403,380	E(DT) TL	30.5 \pm 5.9	W2330(a)
COOS29	4,806,560	398,410	(DT) TL	20.9 \pm 1.4	W3121(a)
COOS31	4,806,340	400,830	E(DP) TL	37.4 \pm 4.1	W3122(a)
COOS37	4,800,020	396,390	E(DT) TL	>65.5 \pm 4.1	W3120(a)
<i>BAND</i>					
BAND6	4,786,210	386,610	W(DB) TL	54.3 \pm 6.4	W3587(a)
BAND9a	4,784,640	386,810	W(DT) TL	39.7 \pm 6.3	W3126(a)
BAND9b	4,784,640	386,810	W(DP) TL	38.1 \pm 3.4	W3127(a)
BAND33	4,771,120	389,650	E(S) TL	111 \pm 9	W3391(a)
BAND47	4,762,470	384,630	(DP) TL	67.3 \pm 21.7	W3391(a)

Table 3 (continued)

Sheet Site	UTM Northing	UTM Easting	Position TL/OSL	Age $\pm 1\sigma$ (ka)	Lab ID (Ref)
<i>GOLD</i>					
GOLD7a	4,702,210	382,800	W(DP) TL	31.1 \pm 6.3	W3588(a)
GOLD7b	4,702,210	382,800	W(DB) TL	54.0 \pm 3.8	W3589(a)
<i>Indian Sands</i>					
35CU674B	4,668,000	387,300	(DT) OSL	35.6 \pm 5.6	–(e)

UTM coordinates are in meters of section 10N, WGS1983.

Luminescence dates include samples dated by thermoluminescence (TL) and Optically-stimulated luminescence (OSL).

Stratigraphic positions of the dated samples are denoted relative to 1) the western W- or eastern E- boundaries of the existing dune sheet, and 2) the Holocene or Pleistocene dune sequence including dune top (DT), internal dune paleosol (DP), or dune base (DB). Samples are also dated from dune ramps at Holocene sea cliffs (DR), dune barrage lakes (DL) which post-date the onset of dune-sheet emplacement, and Pleistocene beachface deposits (S) which pre-date the emplacement of overlying dune sheets.

References: a = Peterson et al. (2006), b = Wiedemann (1990), c = Jungner et al. (2001), d = Heikkinen (1994), e = Davis et al. (2004) and Davis (2006).

dune deposits at each backedge site are identified with respect to the period of emplacement (either Pleistocene (P) or Holocene (H)), the site elevation, and its landward distance from the current shoreline (Table 4). With very-few exceptions the backedge sites represent the highest elevations across the dune sheets. Backedge site elevations range from 14 to 141 m above mean sea level (MSL) for the Pleistocene dune sheets, and from seven to 83 m MSL for the Holocene dune sheets.

The landward distances of the Pleistocene dune-sheet backedges range from 0.1 to 6.9 km (Table 4). The landward distances of the Holocene dune-sheet backedges range from 0.3 to 4.0 km. The dune sheets widths, or maximum backedge distances, vary both on regional and local scales. As previously noted, the greatest dune-sheet widths (3–6 km) are limited to the central dune sheets, including NEWP, FLOR, COOS, and BAND. The regional trends in dune-sheet width are thought to reflect regional sand supply, as discussed in later sections of this paper. Additional work is warranted to establish the relations between sand supply, topography, wind power, and existing vegetation, which probably controlled the local variation of dune migration within the individual dune sheets.

4. Discussion

4.1. Dune-sheet dating

Thirty-six radiocarbon and 46 luminescence dates from the upland dunes of Oregon (Tables 2 and 3) permit the first regional analysis of upland dune ages in Oregon. Jungner et al. (2001) has previously reported on same-site comparisons between OSL and ^{14}C dating techniques at Cape Kiwanda in the Pacific City dune sheet. In this study we compared six TL dates to ^{14}C dates from the same stratigraphic interval or to an assumed regressive shoreface age (~ 120 ka) from a

marine high stand at isotope stage 5e (Peterson et al., 2006). The compared ages generally overlap within one standard deviation unit of error as reported by the dating labs (Table 5). However, we analyze the grouped ^{14}C and TL dune dates separately, due to differences in sampling strategy and potential age range of the two dating techniques.

The ^{14}C and TL dune dates from Tables 2 and 3 are summarized in Table 6. Two dominant periods of dune emplacement are apparent from the summarized age data, i.e., Holocene and Pleistocene, as predicted by Cooper (1958). For computational purposes we divide the Holocene and Pleistocene dates at 10 ka. Only two samples out of the 82 dated samples have ages between 10 and 20 ka. The Holocene dune dates average 3 ka and 5 ka for the ^{14}C and TL techniques, respectively. The younger average age (3 ka) for the radiocarbon group probably reflects the abundance of cultural site dates, which generally post-date dune emplacement age. The TL dates, including dune tops, are taken directly from the dune sand, so they better constrain the age of dune emplacement. As previously noted, the basal ages of dated Holocene dunes range from 3 to 8 ka, and average about 5 ka in the study area. The earliest onset of Holocene dune emplacement dated in the study area occurs at FLOR11 (7.3 \pm 0.6 ka TL) and FLOR12 (7668–7824 $\pm 1\sigma$ cal yr BP).

The grouped, Pleistocene dune dates average 40 and 49 ka from the ^{14}C and TL dating techniques, respectively (Table 6). The averaged Pleistocene dates represent minimums, because some ^{14}C and TL samples exceed potential dating ranges of the dating techniques (Tables 2 and 3). The older average age for the TL-dated samples (49 ka) probably reflects the greater potential age range in the TL dating technique. The bulk of the TL-dated Pleistocene dune sections were emplaced between 70 and 30 ka.

A Quaternary Geologic Units - Newport Dune Sheet

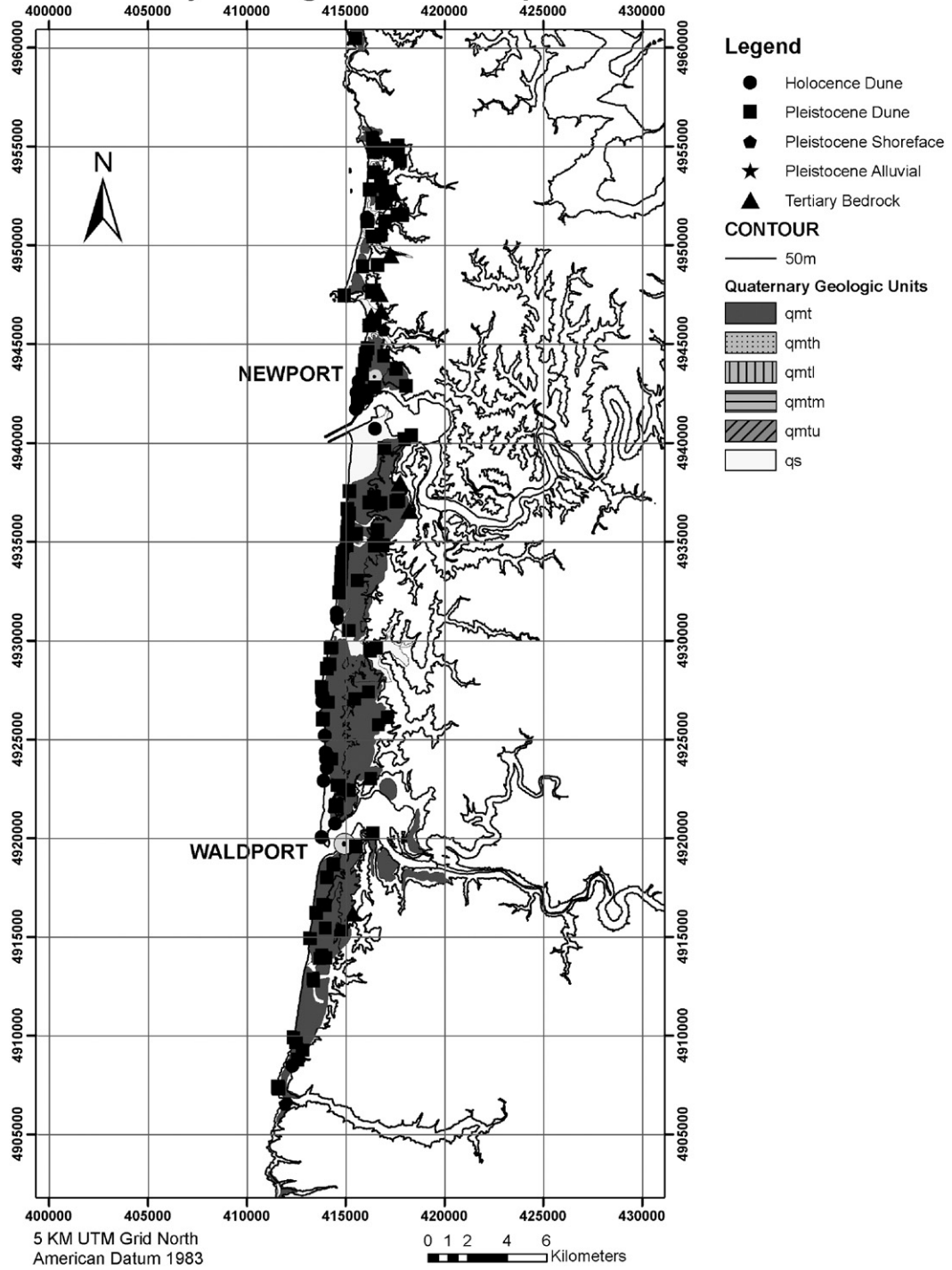


Fig. 3. A Quaternary geology and ground-truth sites of Newport dune sheet, Oregon. B: Quaternary geology and ground-truth sites of Florence dune sheet, Oregon. C: Quaternary geology and ground-truth sites of Coos Bay dune sheet, Oregon. D: Quaternary geology and ground-truth sites of Bandon dune sheet, Oregon.

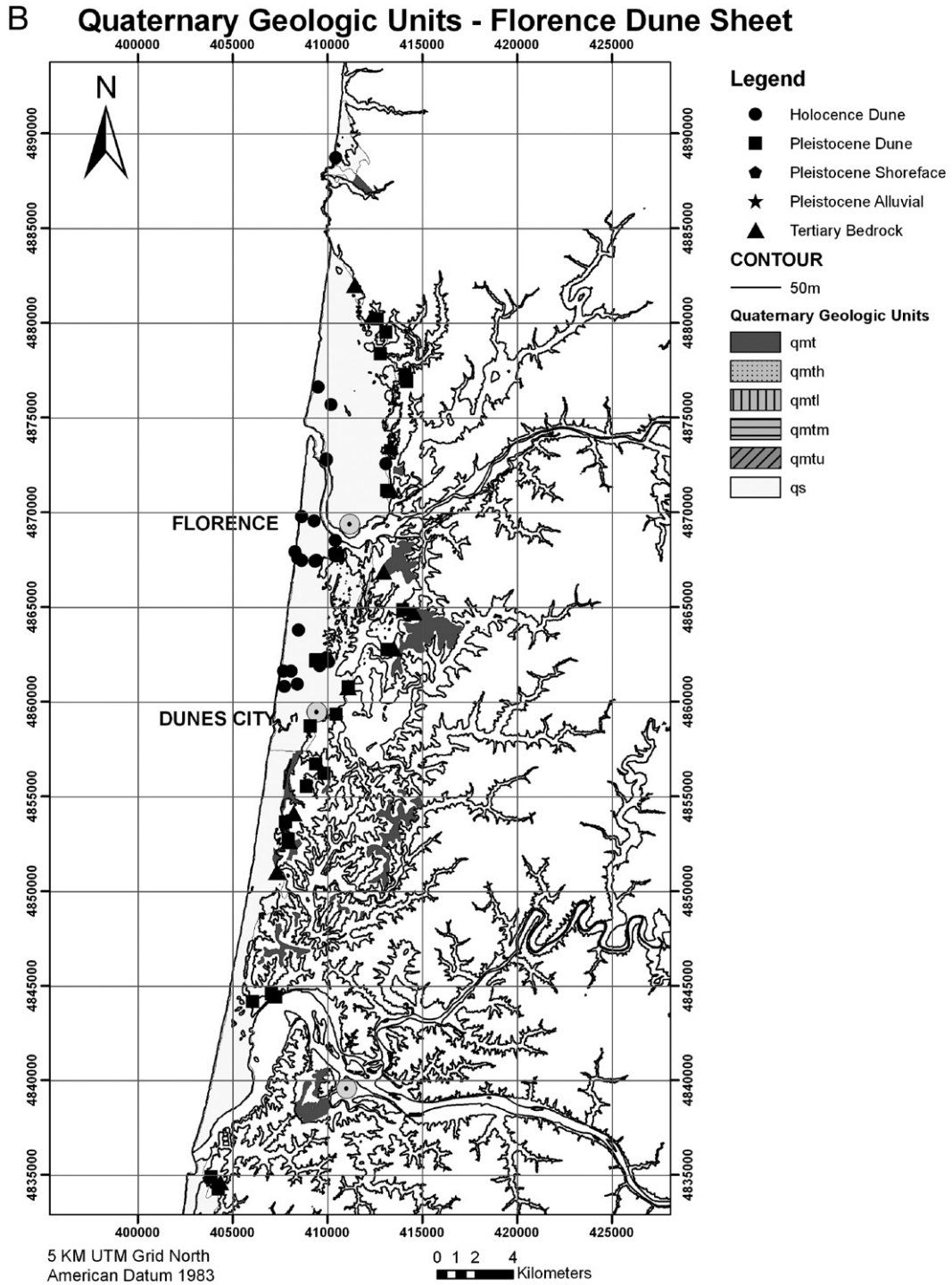


Fig. 3 (continued).

During the course of the study it became apparent that Holocene dunes could be differentiated from Pleistocene dunes on the basis of loess interbeds, topsoil development, and cementation (see Background and

field methods) (Peterson et al., 2006). In an effort to bracket the apparent periods of dune-sheet deposition special attention was made to collecting basal deposits from the Holocene dunes and near surface deposits from

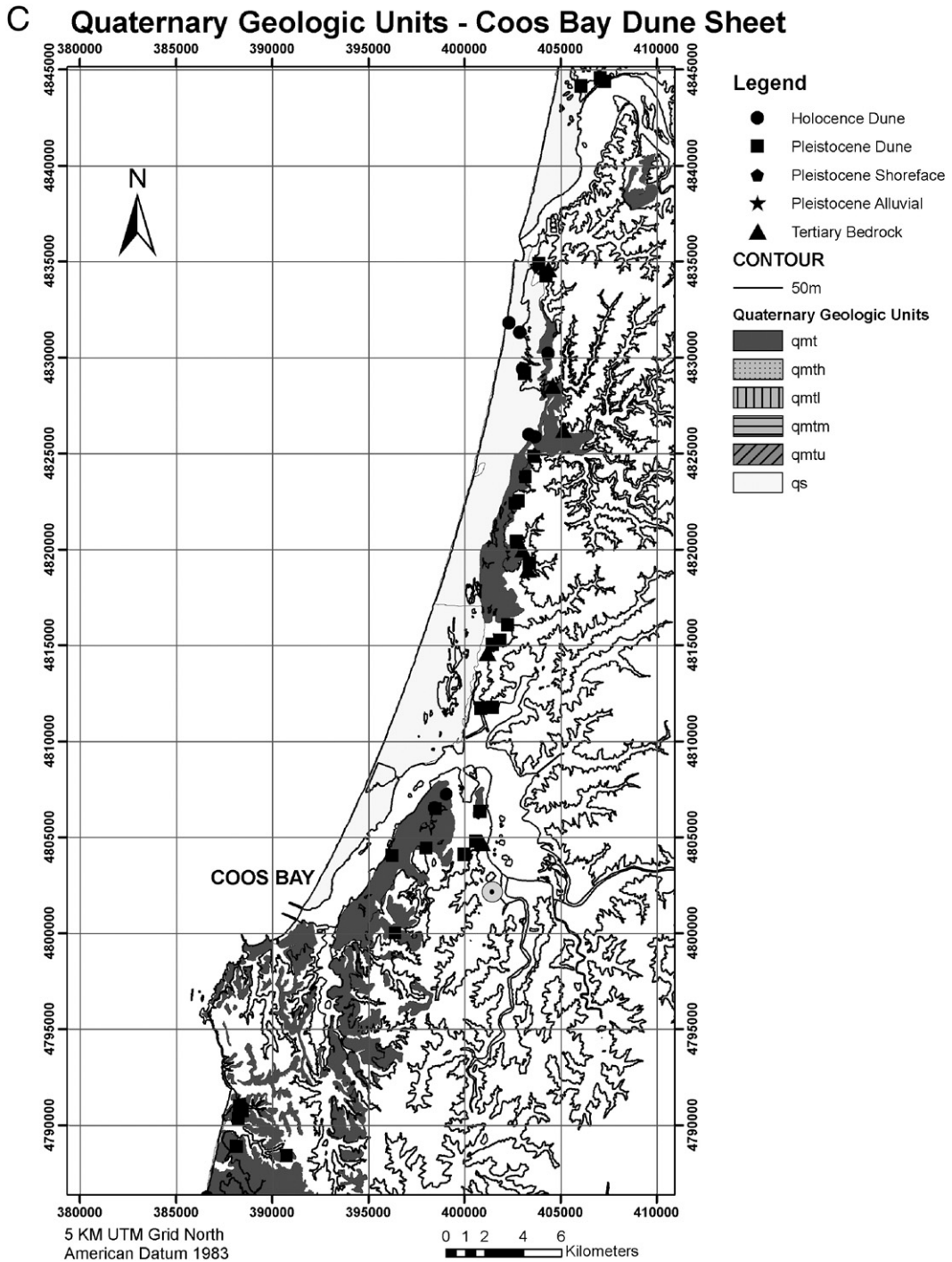


Fig. 3 (continued).

the Pleistocene dune sheets. The general lack of ^{14}C and thermoluminescence dates between 25 and 8 ka was unexpected (Beckstrand, 2001), but it is not thought to be due to sampling gaps. Positive evidence for a hiatus of dune sand supply between 25 and 8 ka is provided by

an anomalously thick, loess paleosol that is widespread in sea cliff exposures between underlying, latest Pleistocene dunes and overlying, earliest Holocene dunes (Hart and Peterson, 2006). The paleosol is time transgressive, extending from deflation-truncated

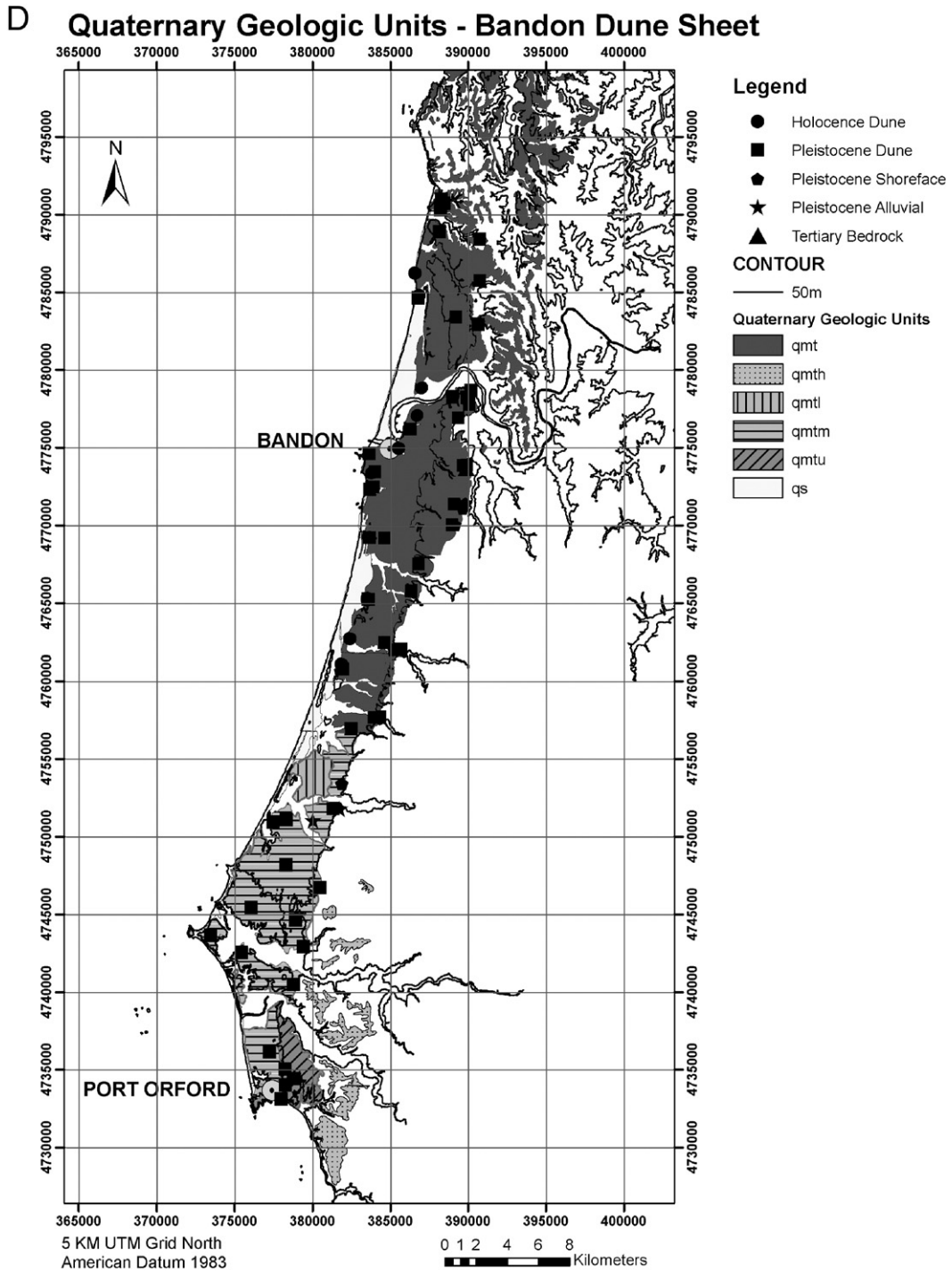


Fig. 3 (continued).

surfaces in the Pleistocene dunes to dune-buried forests that developed on mid-Holocene shore platforms. The duration of development for this hiatus interval is particularly well-constrained in dune deposits at sea cliff sites NEWP103–NEWP82 (46–4 ka), BAND8–

BAND9 (35–2 ka) and GOLD7–GOLD208b (31–6 ka) (Tables 2 and 3).

Two additional dune age gaps appear to include the very-latest Holocene, e.g., younger than 1.5 ka, and the older Pleistocene, e.g., older than 100 ka. The apparent

Table 4
Dune-sheet backedge sites

Sheet-site: period (H/P)	UTM Northing	UTM Easting	Elevation (m MSL)	Landward distance (km)
MANZ2 (H)	5,063,680	427,790	48	1.1
MANZ (H)	5,062,000	428,000	–	1.0
NETA1(P)	5,034,130	424,850	110	0.5
NETA2 (P)	5,033,700	425,120	122	0.7
NETA4 (H)	5,033,240	425,100	73	0.5
NETA8 (H)	5,032,350	425,450	26	0.5
PAC11 (P)	5,019,880	424,670	36	0.5
PAC12 (H)	5,019,550	426,260	75	2.0
PAC13 (P)	5,019,410	424,960	51	0.7
PAC1 (H)	5,015,000	427,000	–	2.5
PAC18 (P)	5,015,420	425,450	7	0.9
PAC118 (H)	5,008,900	424,710	60	0.7
PAC119 (H)	5,006,990	424,870	58	1.0
LINC1 (P)	4,983,930	420,610	37	0.1
LINC6 (P)	4,981,325	421,400	20	1.3
LINC26 (P)	4,976,350	419,870	34	0.6
LINC30 (P)	4,971,200	419,170	35	0.7
LINC32 (P)	4,966,750	417,600	26	0.3
NEWP4 (P)	4,955,050	417,630	112	1.3
NEWP23 (P)	4,951,530	417,870	141	1.8
NEWP32 (P)	4,947,690	416,460	74	1.2
NEWP41 (H)	4,944,790	416,100	25	0.1
NEWP49 (P)	4,942,860	418,060	73	2.4
NEWP50b (H)	4,942,620	415,870	38	0.2
NEWP65 (P)	4,937,090	417,680	99	2.4
NEWP87 (P)	4,933,050	415,570	47	0.8
NEWP105 (P)	4,926,120	417,100	132	3.3
NEWP113 (H)	4,924,010	414,290	12	0.3
NEWP115 (P)	4,923,020	416,270	104	2.4
NEWP123 (H)	4,920,730	414,470	25	0.6
NEWP132 (P)	4,916,200	415,330	25	1.9
NEWP139 (P)	4,913,930	413,700	20	0.6
FLOR (H)	4,882,200	411,300	–	0.3
FLOR3 (P)	4,880,200	412,650	21	3.1
FLOR7 (P)	4,876,900	414,200	136	4.9
FLOR13 (H)	4,872,550	413,090	20	4.0
FLOR14 (P)	4,871,160	413,140	11	4.4
FLOR22 (H)	4,867,680	410,480	35	2.3
FLOR28b (P)	4,864,850	413,990	86	6.1
FLOR42 (P)	4,860,770	411,110	23	3.6
FLOR (H)	4,860,700	410,500	–	3.0
FLOR47 (P)	4,856,200	409,830	55	3.0
FLOR (H)	4,856,000	408,000	–	1.2
FLOR51 (P)	4,852,740	407,950	89	1.5
FLOR55 (P)	4,844,400	407,300	30	2.6
FLOR (H)	4,844,000	405,500	–	0.8
COOS1(P)	4,834,890	403,880	78	1.3
COOS (H)	4,834,000	403,600	–	1.1
COOS6 (H)	4,830,210	404,370	66	2.5
COOS12 (H)	4,825,870	403,690	28	2.7
COOS15 (P)	4,822,540	402,810	91	2.7
COOS (H)	4,820,000	401,500	–	2.2
COOS20 (P)	4,819,270	403,380	46	4.3
COOS28 (H)	4,807,240	399,040	24	2.0
COOS31 (P)	4,806,340	400,830	39	6.3
COOS37 (P)	4,800,020	396,390	91	5.4
BAND2 (P)	4,790,730	388,460	86	1.0
BAND (H)	4,785,000	387,800	–	1.0

Table 4 (continued)

Sheet-site: period (H/P)	UTM Northing	UTM Easting	Elevation (m MSL)	Landward distance (km)
BAND12 (H)	4,778,850	387,000	7	2.0
BAND11 (P)	4,782,940	390,640	27	3.9
BAND17 (H)	4,777,100	386,690	20	2.1
BAND23 (P)	4,773,900	389,910	116	6.9
BAND36 (H)	4,769,260	383,610	15	0.4
BAND40 (P)	4,765,800	386,350	60	4.1
BAND43 (H)	4,765,200	383,550	15	1.5
BAND44 (P)	4,762,030	385,690	106	4.4
BAND48 (H)	4,761,110	381,880	14	1.0
BAND56 (P)	4,751,080	378,320	13	1.3
BAND68 (P)	4,734,420	378,780	85	2.6
GOLD2 (P)	4,711,350	385,960	106	0.5
GOLD5 (P)	4,703,870	383,710	67	0.9
GOLD7 (H)	4,797,370	384,220	20	0.1
GOLD10 (P)	4,698,760	382,450	27	0.3
CROO1 (H)	4,679,500	384,650	67	0.7
CROO2 (H)	4,678,830	384,840	83	1.0
CROO3 (H)	4,678,710	384,730	71	1.0

UTM coordinates are in meters of section 10N, WGS1983.

Period = Holocene (H) or Pleistocene (P).

Elevation = meters above mean sea level (MSL) WGS1983 Datum.

Landward distance = due east distance of site from shoreline in kilometers.

lack of substantial sand supply to the coastal dunes during the last one to two thousand years is possibly related to a widespread truncation of sea cliff dune ramps in the study area (Hart and Peterson, 2006). The long-term loss of sand from many of the study area beaches is under investigation. The lack of Pleistocene dunes with TL ages greater than 100 ka, could be biased by TL saturation in the dune sand grains (Aitken, 1985). However, the lack of dune-sheet cover on the older uplifted marine terraces, and the lack of severely weathered dune deposits in the study area are perplexing. We do not know what limits the apparent ages of the

preserved dune deposits to less than the age of the higher preserved marine terraces, e.g., possibly isotope stage 7 at about 200 ka.

4.2. Sea-level control on periods of dune emplacement

The two dominant periods of dune emplacement, as summarized in Table 6, fall into late-Pleistocene conditions of marine low-stand, and middle-to-late-Holocene conditions of marine high stand (Table 6 and Fig. 4) (Chappell and Shackleton, 1986; Pirazzoli, 1993). Most

Table 5
Comparison of TL dates, radiocarbon, and marine terrace ages

Site ID	Radiocarbon	5e Regressive	Measured TL
Position (UTM-N)	RCYBP $\pm 1\sigma$	Shoreface (\sim ka)	(ka $\pm 1\sigma$)
NEWP86	3600–3720	–	–
NEWP82	–	–	4.1 \pm 0.4
NEWP103b	–	\sim 120	111 \pm 23
FLOR12	7670–7822	–	–
FLOR11	–	–	7.3 \pm 0.6
FLOR54	>45,300	–	–
FLOR56	–	–	45.3 \pm 3.1
BAND9	35,400– 36,200	–	–
BAND9b	–	–	38.1 \pm 3.4
BAND33	–	\sim 120	111 \pm 9

Sample ages, i.e. radiocarbon or TL are from Tables 2 and 3. Shoreface age from the Pioneer terrace (isotope stage 5e high stand). Regressive deposits assumed to post-date high stand by \sim 5 ka.

Table 6
Summary of Oregon dune-sheet ages

Group method	Number of samples	Minimum age (ka)	Maximum age (ka)	Average age (ka)
Holocene radiocarbon	30	0	8	3
Pleistocene radiocarbon	6	29	>47	40*
Holocene luminescence	16	0.4	7.3	5
Pleistocene luminescence	29	11	103	49*

The dune dates are grouped by dating method, i.e., either radiocarbon or luminescence, and by period, i.e., either Holocene (<10,000 RCYBP) or Pleistocene (>10,000 RCYBP).

*The average ages for the Pleistocene dunes represent minimum values. Some samples exceeded the commercial range of radiocarbon dating (Table 2) or were saturated with respect to thermoluminescence (Table 3).

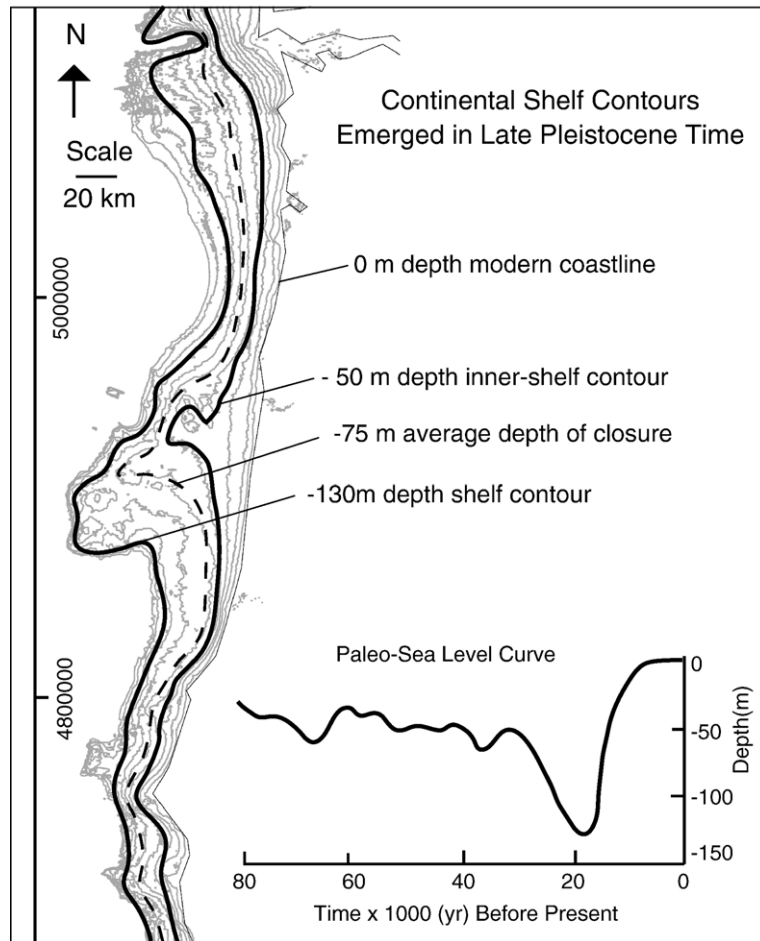


Fig. 4. Map of Oregon continental shelf showing paleo-sea levels (solid lines) at -50 m and -130 m isobaths. A eustatic, sea-level curve is shown for the last 80,000 years (figure redrafted from Pirazzoli, 1993, sea-level curve from Chappell and Shackleton, 1986). The major period of Late-Pleistocene dune emplacement (30–70 ka) is dominated by sea levels of about 50 m below present sea level. The average depth of closure, e.g., limit of littoral transport (dashed line at -75 m contour), for the late Pleistocene is assumed to have been about 25 m below the average sea level for that period. Sea level during the last glacial maximum (21–18 ka) briefly decreased to 130 m below present sea level.

of the Pleistocene dune dates, e.g., within 50 ± 20 ka, occur during sea levels that were generally 50 m below present level. Due to a relatively deep depth of closure on this high-wave energy coast (20–30 m below sea level) the maximum depth of littoral transport should be 20–30 m below the corresponding former sea level. During the lowered sea-level conditions the inner-continental shelf, presently extending to 50 m below sea level, was emerged and exposed to eolian processes. Onshore wind transported sand across the shelf to the foothills of the coast range, where deposits accumulated for tens of thousands of years. Dry and cool coastal conditions during the latest Pleistocene (Worona and Whitlock, 1995; Griggs and Whitlock, 1997) should have limited vegetative stabilization, further promoting the across-shelf transport of sand by eolian processes. Numerical

models of late-Pleistocene wind directions are discussed below. Broad eolian dune and/or deflation surfaces were located offshore of the largest dune sheets NEWP, FLOR, COOS, BAND. These low-stand dune sheets extended right across the inner-shelf from 80 to 10 ka.

Unlike dune deposits from the southern California coast (Orme, 1992; Erlandson et al., 2005) the Oregon dune sheets lack a significant number of emplacement dates from the last glacial maximum (LGM), e.g., 21–18 ka (Tables 2 and 3). At that time the sea level briefly fell to about 130 m below the present level (Fig. 4). Such low sea levels should have exposed most of the middle shelf, providing abundant fine sand sources for eolian transport (Beckstrand, 2001). However, little dune-sheet emplacement occurred during the LGM period in Oregon. Onshore wind power in coastal Oregon might

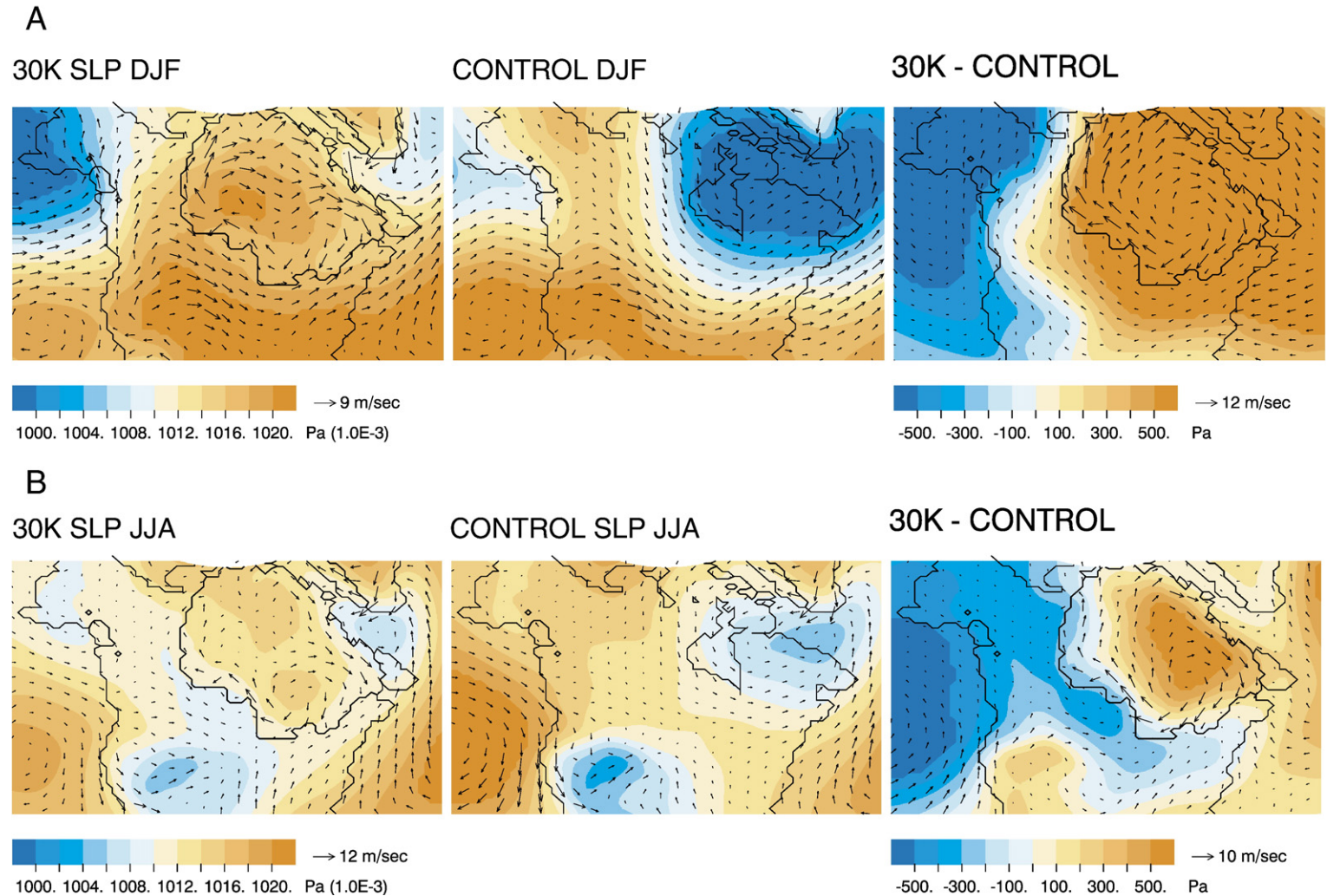


Fig. 5. A–D: Modeled sea-level pressure (SLP) and associated wind flow (vectors) for time periods (30 ka, 21 ka and 0 ka) and seasons including winter months, December, January and February (DJF) and summer months June, July and August (JJA). Part A is 30 ka Winter months (left panel), control 0 ka Winter months (center panel), and past–present difference Winter months (right panel). Part B is for the same 30 ka and 0 ka time periods but shows the modeled paleoclimate data for the summer months. Part C and D are 21 ka and 0 ka time periods, with Winter months in Part C and summer months in Part D. Sea-level pressure (SLP) in 10^{-3} Pa units, ranges from 1000 to 1020. Wind vectors reach maximum, average velocities of $9\text{--}12\text{ ms}^{-1}$.

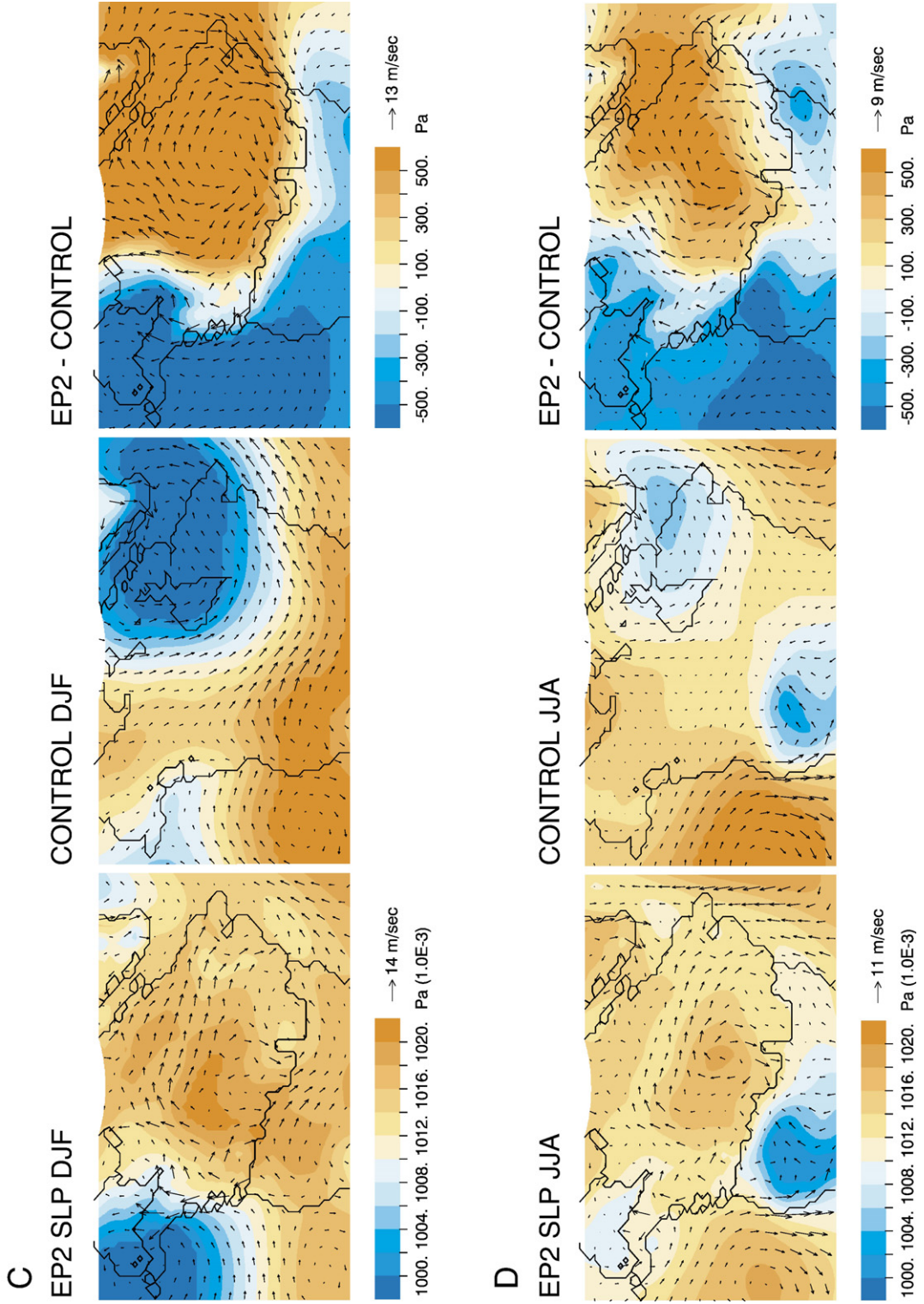


Fig. 5CD (continued).

have been reduced during the LGM due to anticyclonic wind flow off the Laurentide ice sheet and/or reduced, offshore high pressure during the summer months (see discussion of modeled LGM wind flow below).

4.3. Modeled paleoclimate sea-level pressure and wind flow

Numerical models of sea-level pressure (SLP) and associated wind flow vectors are shown for North America during the latest Pleistocene, e.g., 30 ka (Fig. 5A,B) and the LGM at 21 ka (Fig. 5C,D). The modeled conditions are averaged for winter (DJF) and summer (JJA) months. The modeled, late-Pleistocene conditions are compared to modern 0 ka (control) conditions by differencing, yielding past–present difference anomalies. The details of these model runs are presented elsewhere (Patrick and Hostetler, 2004). The paleoclimate model step at 30 ka (Fig. 5A,B) is chosen to represent the intermediate, ice age conditions that would have predominated between 70 and 30 ka. That is the interval that is most frequently represented by the Pleistocene dune emplacement dates (Table 6). The model step at 21 ka (Fig. 5C,D) is thought to represent LGM conditions of maximum, ice sheet extent and moderated, land–sea pressure gradients.

Based on the modeled SLP during the 30 ka model step the NE Pacific low-pressure margin, for example the 1004×10^{-3} Pa contour, extended 500–1000 km south of its present, average winter position (Fig. 5A, left and center panels). Winter winds in the late Pleistocene had more southerly origins, relative to present conditions (Fig. 5A, difference anomaly in right panel), which would have generated winter waves with more southerly directions relative to the present. The more oblique wave attack on the north–south trending coastline would have enhanced northward littoral drift, during winter months of maximum wave energy. The enhanced northward littoral drift, as predicted from the modeled 30 ka winter wind vectors, is consistent with the net northward dispersal of trace minerals in Oregon continental shelf deposits (Schiedegger et al., 1971).

During summer months the modeled 30 ka pressure gradient between the offshore high pressure and onshore low-pressure centers was greatly reduced, relative to present conditions. Such weak pressure gradients would have yielded very-weak winds and very-small waves out of the northwest compared to modern summer conditions (Fig. 5B, see differencing anomaly in right panel). Net northward littoral drift would have completely dominated the low-stand shorelines of northernmost California and Oregon during the late Pleistocene.

Modeled SLP and associated wind conditions during the LGM at 21 ka (Fig. 5C,D) show even greater differences from modern wind forcing along the coasts of northern California and Oregon. The NE Pacific low-pressure margin, e.g., 1004×10^{-3} Pa, descends to the USA and Canadian border latitude, yielding southerly, average winter winds along the coast as far south as central California. The southward displacement of winter storm tracks, to the central California latitudes, is confirmed by studies of increased landsliding and temperate forest pollen prior to 12 ka, relative to the drier and more stable scrubland conditions that have predominated on the central California coast since 10 ka (Reneau et al., 1986; Rypins et al., 1989).

Modeled, winter wind vectors along the Oregon coast during the LGM are directed nearly due north, due to a combination of low-pressure offshore and anticyclonic flow off the interior high pressure area over the Laurentide ice sheet. The modeled, summer SLP gradient across the Oregon coast is further reduced during the LGM, relative to the previous late-Pleistocene period. Both of the conditions above would have substantially diminished the onshore wind power needed to migrate dunes across the broadly-emerged continental shelf in Oregon during the LGM.

Following the LGM, a rapid rise of sea level, that is the early-Holocene marine transgression (Fig. 4), was well underway by 16 ka in the region (Baker et al., *in press*). The transgression had reached the 50 m isobath by 10 ka, and the 10–15 m isobath by 7.5 ka. The marine transgression submerged the inner-continental shelf between 10 and 7.5 ka, thereby terminating any potential eolian transport across the shelf. During the early-Holocene transgression the shoreline migrated landward at rates of about 10 m per year, which outdistanced the onshore transport of sand by ocean waves. As the rate of sea-level rise declined after 9 ka (Fig. 4) the onshore transport of sand by ocean waves was sufficient to deliver a surplus of sand to the shoreline. The earliest onset of Holocene dune emplacement in the study area dates to 8–7 ka (Tables 2 and 3). Littoral processes continued to deliver sand to the beaches for several thousand years, as evidenced by Holocene dune-sheet dates that average 3–5 ka in age (Table 6).

At the present time the mean winter storm track in the northeast Pacific intersects the central Oregon coast (Peterson et al., 1990; Fig. 5, central panel). There is no reported net-littoral drift near the landfall of the mean winter storm track in the central Oregon coast (Komar et al., 1976). Winter, average wind vectors are strongly oriented onshore and the summer offshore-to-onshore

SLP gradient is at maximum strength during the present period (Fig. 5, central panel). Onshore wind power peaked during the Holocene to migrate dunes inland from the high-stand beach strandlines.

4.4. Low-stand depocenter

The along-coast distributions of late-Pleistocene and Holocene dune sands are summarized by proxies taken from the corresponding backedge sites (Table 4). Specifically, the backedge site data are averaged to calculate dune-sheet length, landward elevation, width, and surface area for each of the late-Pleistocene and Holocene dune sheets (Table 7).

Averaged landward elevations of the central Pleistocene dune sheets (NEWP to BAND) range from 56 to 83 m elevation above mean sea level (Table 7). The large dune sheets climbed over uplifted marine terraces and filled small valleys. By comparison, the central Holocene dune sheets average only 14 to 39 m elevation, where they overlap the broader deflation aprons of the Pleistocene dune sheets. The narrow parabolic dunes at opposite ends of the study area, such as PACI and CROO, average 64 to

Table 7
Emplacement period and size of Oregon upland dune sheets

Dune-sheet name	Mid-point location UTM-N	Nominal length N–S (km)	Average elevation (m MSL)	Average width E–W (km)	Surface area (km ²)
<i>Pleistocene (low stand)</i>					
MANZ	–	–	–	–	–
NETA	5,033,915	0.5	–	0.6	0.5
PACI	5,017,650	4.5	31	0.7	3
LINC	4,975,340	12	30	0.6	7
NEWP	4,934,490	28.5	83	1.7	35
FLOR	4,862,300	36	56	3.6	130
COOS	4,817,455	35	69	4.0	139
BAND	4,762,575	56	70	3.5	196
GOLD	4,705,055	12.5	67	0.5	6
CROO	–	–	–	–	–
Total	–	–	–	–	516
<i>Holocene (high stand)</i>					
MANZ	5,062,840	1.7	–	1.1	2
NETA	5,032,795	0.9	–	–	0.5
PACI	5,017,275	12.5	64	1.5	19
LINC	–	–	–	–	0
NEWP	4,932,760	5.5	25	0.3	2
FLOR	4,863,100	38.5	27	1.9	73
COOS	4,820,620	27	39	2.1	57
BAND	4,773,055	23.5	14	1.3	30
GOLD	4,702,210	0.1	20	0.1	0.1
CROO	4,679,105	1	73	0.9	1
Total	–	–	–	–	184

Data used in calculations are from Table 4.

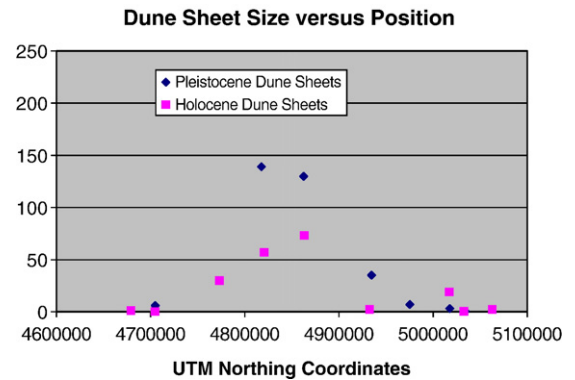


Fig. 6. Plots of Pleistocene and Holocene dune-sheet size (km²), in surface area, relative to positions along the Oregon coast (500 km coastline length). Both Holocene and Pleistocene dune sheets dramatically increase in size in the south-central coast (48⁰⁰–49⁰⁰ UTM-northings). Dune-sheet names and map positions are shown in Fig. 1.

73 m elevation respectively, where they ramp up against prominent headlands. Unlike lowland dune sheets in barrier spits and prograded coastal plains (Cooper, 1958), the upland dune sheets are not restricted to low-relief coastal topography.

Dune-sheet thicknesses (2–50 m thick) in measured profiles and boreholes (Peterson et al., 2006) are poorly constrained in most of the dune sheets. However, dune-sheet widths are well-established from mapping the dune-sheet backedges (Tables 4 and 7). The central Pleistocene dune sheets, from NEWP to BAND, range from 2.7 to 4.0 km in average width. By comparison, the corresponding Holocene dunes sheets reach about one half of those widths, yielding west–east distances of only 0.3 to 2.1 km. Unlike the Holocene dune sheets, the late-Pleistocene dune sheets extended across the inner-shelf. Their widths during low-stand conditions varied as a function of shelf gradient, but locally exceeded 20 km in shore-normal distance (Figs. 1 and 4).

Existing dune-sheet surface area is used as a proxy for dune sand volume in this regional study. The late-Pleistocene dune sheets range from less than one to nearly 200 km² in surface area (Table 7). The three largest dune sheets, including FLOR, COOS and BAND, account for 90% of the Pleistocene dune-sheet cover in the study area. The Holocene dune sheets are substantially smaller, ranging from 1 to 57 km² in surface area. The three largest, dune sheets, including FLOR, COOS and BAND, also represent 87% of the total Holocene dune cover. About 90% of the dune sand supply in both Pleistocene and Holocene time was distributed over a 130 km coastal reach that was centered in the south-central Oregon coast (Fig. 6).

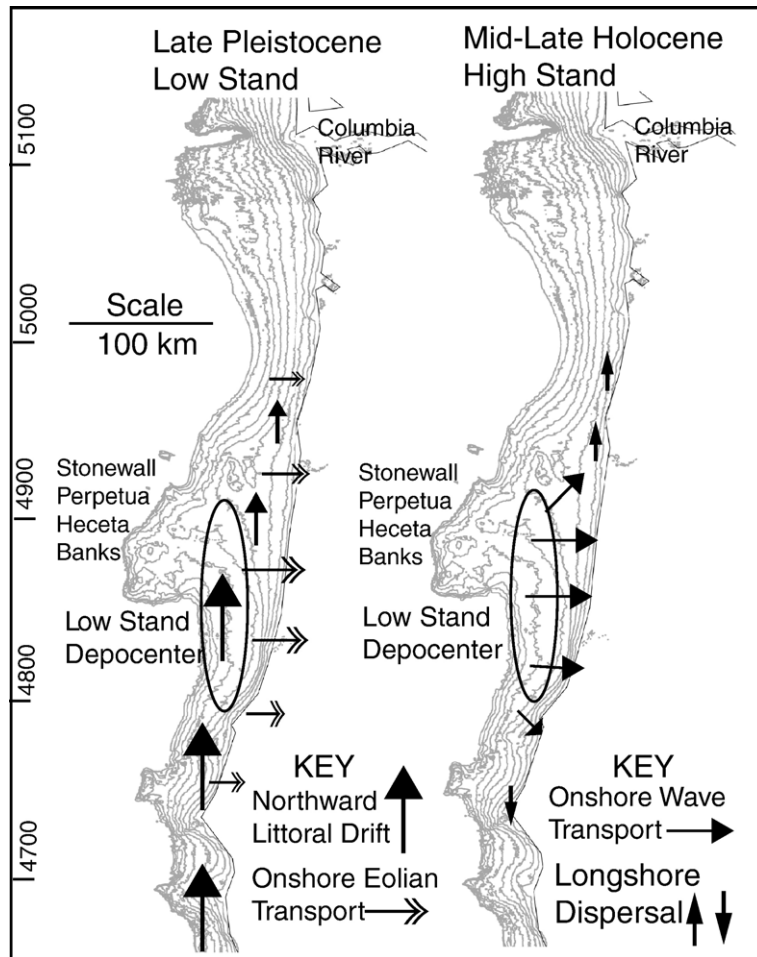


Fig. 7. Diagram of coastal sand transport during late-Pleistocene 'low-stand' conditions (left side) and coastal sand transport during mid-Holocene 'high-stand' conditions (right side). Magnitude of sand transport is diagrammatically represented by arrow size. Shelf bathymetry is shown in 20 m isobaths. The late-Pleistocene depocenter is located just south of the Stonewall, Perpetua, and Heceta (SPH) Banks complex.

The dominant accumulation of dune sand in the south-central Oregon coast corresponds to an abrupt widening of the continental shelf at the Stonewall, Perpetua and Heceta Banks (Figs. 4 and 7). The south margin of the Bank complex deflects the 50 m isobath by about 30–40° to the west, and the 100 m isobath by 60–70° west. Under low-stand conditions the emerged Stonewall, Perpetua and Heceta (SPH) Banks produced a large coastal bight that largely blocked northward littoral transport. Large volumes of sand were trapped in a low-stand depocenter that was located south of the SPH Banks complex. Onshore winds transported the depocenter sand across the continental shelf to the present Pleistocene dune fields. Fluctuating sea levels, and/or northeast eolian transport, permitted small amounts of littoral sand to bypass the SPH Banks. Minor shelf deposits north of the Banks fed the small,

northern Pleistocene dune sheets (PACI, LINC, NEWP) (Table 7) during the late-Pleistocene low stand.

Although the northernmost California Rivers are characterized by very-high sediment discharge (Peterson et al., 1991), no significant Pleistocene dune sheets developed there. The northern California coast is characterized by a narrow shelf, which is dissected by submarine canyons. The sand that was retained on the narrow shelf was transported north to the SPH Banks depocenter, leaving the northernmost California coast stripped of offshore sand sources.

The Holocene marine transgression reworked the accumulated deposits in the SPH Banks low-stand depocenter, which included the broad Pleistocene dune sheets that traversed the inner-shelf. Wave transport moved the depocenter sand landward to develop beaches near the present shorelines (Fig. 7). By mid-

Holocene time (8–7 ka) the abundant sand supply and onshore wind power led to the onset of Holocene dune emplacement. The great concentration of Holocene dune sand, located due east of the low-stand SPH Banks depocenter (Figs. 6 and 7), indicates relatively little longshore dispersal during shoreward transport.

However, the smaller dune sheets at the northern ends of the study area show some interesting longshore anomalies. For example, the terminal dune sheets, including MANZ and CROO, are larger than neighboring dune sheets, and the PACI dune sheet at 19 km² is much larger than either of its adjacent dune sheets (0–2 km²) (Table 7). These late-Holocene dune fields (Tables 2 and 3) might reflect the secondary effects of longshore transport following the Holocene transgression. Additional work is underway to use the ages and longshore distribution of the small Holocene dune fields to establish net-littoral drift in northernmost and southernmost Oregon during the late-Holocene high stand.

The broad dune sheets and sandy beaches of the south-central Oregon coast owe their origins to the direct onshore transport of sand from the SPH Banks low-stand depocenter. Similar low-stand depocenters might be responsible for large coastal dune sheets in central and southern California (Cooper, 1967; Bonilla, 1971; Dupre, 1975; Orme, 1992) and the southern Baja Peninsula (Murillo De Nava et al., 1999) (Fig. 1) among other continental margins. The dating of pre-Holocene dunes in those large, coastal dune sheets should test their potential origins from offshore depocenters that formed during low-stand conditions.

5. Conclusions

The upland coastal dunes in Oregon fall into two periods of emplacement including marine low-stand conditions during the late-Pleistocene and marine high-stand conditions during the middle- to late-Holocene. Sea-level low stands exposed the inner-continental shelf to eolian transport by onshore wind during late-Pleistocene time. Late-Pleistocene dune sheets traversed the inner-continental shelf and ramped onto the foothills of the coast range.

The lack of substantial dune emplacement in Oregon during the last glacial maximum (LGM) is thought to possibly reflect anticyclonic flow off the Laurentide ice sheet, and/or diminished across-margin pressure gradients that briefly reduced onshore wind power in Oregon. With the ensuing Holocene transgression the inner-shelf was submerged, thereby terminating the eolian cross-shelf sand supply. Following the decline in rate of sea-

level rise during the middle-Holocene the onshore wave transport delivered inner-shelf sand to the beaches. Peak onshore wind velocities during the Holocene permitted the eolian transport of surplus littoral sand inland to form the upland, Holocene dune sheets.

The large, upland dune sheets in south-central Oregon are not controlled by modern shoreline topography, nor are they directly associated with large rivers. The largest dune sheets of both late-Pleistocene and Holocene age occur just south and landward of a prominent offshore bank complex, named the Stonewall, Perpetua, and Heceta (SPH) Banks. During late-Pleistocene conditions of marine low stand the emerged SPH Banks blocked northward littoral drift on the continental shelf. The littoral sand accumulated south of the SPH Banks forming a large low-stand depocenter. The low-stand depocenter supplied sand to the large late-Pleistocene dune sheets via eolian cross-shelf transport.

During the Holocene transgression the inner-shelf sand deposits were remobilized by onshore wave transport. The large Holocene dune sheets reflect the surplus sand supplied to the south-central Oregon beaches by eastward wave transport. Only small, Holocene dune fields occur north and south of the low-stand depocenter. Limited longshore transport by littoral processes during late-Holocene times might have continued to supply the smallest, upland dunes at the northernmost and southernmost ends of the Oregon coast study area.

Acknowledgements

We thank Ralph Hunter, Mark Darienzo, Courtney Cloyd, Darren Beckstrand, and Peter Cowell for stimulating discussions about the possible origins of the Oregon Dunes. David Percy performed GIS map compilations of coastal, Quaternary geologic units and modern shelf bathymetry. Rick Minor and Loren Davis supplied unpublished or recently published dates from cultural sites in the coastal dunes. This research on coastal dune landscapes of the central west coast of North America was funded by the NOAA Office of Sea Grant and Extramural Programs, U.S. Department of Commerce, under grant number NA76RG0476, project number R/SD-04, and by appropriations made by the Oregon State Legislature. Additional dating of dune deposits from the Oregon Dunes National Recreation Area (ODNRA) was supported by the Siuslaw National Forest. Further dune dating support and analysis was provided by Griffith University, Brisbane, Queensland, Australia, and Wollongong University, Wollongong, New South Wales, Australia.

References

- Aitken, M.J., 1985. Thermoluminescence dating. *Studies in Archaeological Science*. Academic Press, London. 359 pp.
- Aitken, M.J., 1998. An Introduction to optical dating. The dating of Quaternary sediments by the use of photon stimulated luminescence. Oxford University Press, New York. 267 pp.
- Baker, D., Peterson, C., Twichel, D., Hemphill-Haley, E., Holocene sedimentation in the Columbia River Estuary, *Marine Geology*, in press.
- Bannan, J.G., 1989. Sand Dunes. Carolrhoda Books, Inc., Minneapolis. 47 pp.
- Beaulieu, J.D., Hughes, P.W., 1975. Environmental geology of western Coos and Douglas Counties, Oregon. State of Oregon Department of Geology and Mineral Industries, Bulletin 87, 148 p. with maps.
- Beaulieu, J.D., Hughes, P.W., 1976. Land use geology of western Curry County, Oregon. State of Oregon Department of Geology and Mineral Industries, Bulletin 90, 148 p. with maps.
- Beckstrand, D.L., 2001. Origin of the Coos Bay and Florence dune sheets, south central coast, Oregon. Unpublished M.S. thesis, Portland State University, Portland, Oregon, 192 p.
- Bonilla, M.G., 1971. Preliminary geologic map of San Francisco South quadrangle and part of the Hunters Point quadrangle, California. U.S. Geological Survey Miscellaneous Field Studies Map MF-311, 1:24,000.
- Briggs, G.G., 1994. Coastal crossing of the elastic strain zero-isobase, Cascadia margin, south-central Oregon coast. M.S. Thesis, Portland State University, Portland, Oregon, 251 p.
- Clark, L.A., 1991. Archaeology of seal rocks (35LNC14). Prehistory of the Oregon Coast: The Effects of Excavation Strategies and Assemblage Size on Archaeological Inquiry, by R. Lee Lyman, pp. 175–240.
- Carlson, J., Reckendorf, F., Temyik, W., 1991. Stabilizing coastal sand dunes in the Pacific Northwest. United States Department of Agriculture, Soil Conservation Service, Agriculture Handbook, vol. 687. 53 pp.
- Chappell, J., Shackleton, N.J., 1986. Oxygen isotopes and sea level. *Nature* 324, 137–140.
- Clemens, K.E., Komar, P.D., 1988. Oregon beach sand compositions produced by mixing of sediments under a transgressing sea. *Journal of Sedimentary Petrology* 58, 519–529.
- Cooper, W.S., 1958. Coastal sand dunes of Oregon and Washington. *Geology Society of America Memoir* 72. 169 pp.
- Cooper, W.S., 1967. Coastal dunes of California. *Geology Society of America Memoir* 104. 131 pp.
- Davis, L.G., 2006. Geoarchaeological insights from Indian Sands, a late Pleistocene site on the southern Northwest Coast. *Geoarchaeology: Int. J.* 21, 351–361.
- Davis, L.G., Punke, M.L., Hall, R.L., Filmore, M., Willis, S.C., 2004. Evidence for a late Pleistocene occupation on the southern coast of Oregon. *Journal of Field Archaeology* 29 (1), 7–16.
- Dupre, W.R., 1975. Maps showing geology and liquefaction potential of the Quaternary deposits in Santa Cruz County, California: U.S. Geological Survey Misc. Field Studies Map, MF-643, 2 sheets, scale 1:62,500.
- Erlandson, J.M., Tveskov, M.A., Byram, R.S., 1998. The development of maritime adaptations on the southern northwest coast of North America. *Arctic Anthropology* 35, 6–22.
- Erlandson, J.M., Rick, T.C., Peterson, C., 2005. A geoarchaeological chronology of Holocene dune building on San Miguel Island, California. *Holocene* 15, 1227–1235.
- Grathoff, G., Peterson, C., Beckstrand, D.L., 2003. Coastal dune soils in Oregon, USA, forming allophane and gibbsite. 2001. A Clay Odyssey, Proceedings to the 12th International Clay Minerals meeting Bahia Blanca, Argentina, pp. 197–204.
- Griggs, L.D., Whitlock, C., 1997. Late-glacial vegetation and climate change in western Oregon. *Quaternary Research* 49, 287–298.
- Hart, R., Peterson, C., 2006. Late Holocene buried forests on the Oregon coast. *Earth Surface Processes and Landforms* 32, 21–220. doi:10.1002/esp.1393.
- Heikkinen, O., 1994. The Pacific Northwest coastal dunes — human influence and natural changes. *Terra* 106 (3), 267–276.
- Jungner, H., Korjonen, K., Heikkinen, O., Wiedemann, A.M., 2001. Luminescence and radiocarbon dating of a dune series at Cape Kiwanda, Oregon, USA. *Quaternary Science Reviews* 20, 811–814.
- Komar, P.D., Lizarraga-Arciniega, J.R., Terich, T.A., 1976. Oregon coast shoreline changes due to jetties. *Journal of the Waterways Harbors, and Coastal Engineering Division*. Proceedings of the ASCE, vol. 102, no. WW1, pp. 13–30.
- Minor, R., 1991. Yaquina head: a middle archaic settlement on the north-central Oregon coast, Bureau of Land Management, cultural resource manual No. 6. Natural Resource Conservation Service, 1997, Soil Survey of Lincoln County Area, Oregon.
- Minor, R., 2006. Archaeological Testing at Prehistoric Site 35TI74, Cape Lookout State Park, Tillamook County, Oregon. Field records on file at Heritage Research Associates, Eugene, Oregon.
- Minor, R., Toepel, K.A., 1986. The archaeology of the Tahkenitch landing site: early prehistoric occupation on the Oregon coast. Heritage Research Associates Report No. 46, Eugene.
- Minor, R., Greenspan, R.L., Hughes, R.E., Tasa, G.L., 2000. The Siuslaw dunes. In *Changing Landscape: Proceedings of the 3rd Annual Coquille Cultural Preservation Conference*, 1999. R.J., Losey. Coquille Indian Tribe, North Bend, Oregon, pp. 82–102.
- Moss, M., Erlandson, J., 1995. An evaluation, survey, and dating program for archaeological sites on state lands of the Northern Oregon Coast. Report on file, Oregon State Historic Preservation Office, Salem.
- Muhs, D.R., Kelsey, H.M., Miller, G.H., Kennedy, G.L., Whelan, J.F., McInelly, G.W., 1990. Age estimates and uplift rates for late Pleistocene marine terraces: Southern Oregon portion of the Cascadia forearc. *Journal of Geophysical Research* 95, 6685–6698.
- Murillo De Nava, J.M., Gorsline, D.S., Goodfriend, G.A., Vlasov, V.K., Cruz-Orozco, R., 1999. Evidence of Holocene climatic changes from Aeolian deposits in Baja California Sur, Mexico. *Quaternary International* 56, 141–154.
- Musil, R.R., 1998. Age of the Hauser Site. In *The Hauser Site: Archaeological Evidence of a Paleo-Estuary in the Oregon Dunes, South-Central Oregon Coast*, by Rick Minor and Ruth L. Greenspan. Report to the Siuslaw National Forest, Corvallis, pp. 71–78.
- Orme, A.R., 1992. Late Quaternary deposits near Point Sal, South-Central California: a time frame for coastal dune emplacement. In: Fletcher, C.H., Wehmiller, J.F. (Eds.), *Quaternary Coasts of the United States: Marine and Lacustrine Systems*, IGCP Project #274. Society for Sedimentary Geology, Special Publication, vol. 48, pp. 310–315.
- Patrick, B.J., Hostetler, S.W., 2004. Modeling paleoclimates. In: Gillespie, A.R., Porter, S.C., Atwater, B.F. (Eds.), *The Quaternary period in the United States*. [Serial] *Developments in Quaternary Science*, vol. 1, pp. 565–584.
- Peterson, C.D., Jackson, P.L., Oneil, D.J., Rosenfeld, C.L., Kimmerling, A.J., 1990. Littoral cell response to interannual climatic forcing 1983–1987 on the central Oregon coast, USA. *Journal of Coastal Research* 6, 87–110.
- Peterson, C.D., Darienzo, M.E., Pettit, D.J., Jackson, P., Rosenfeld, C., 1991. Littoral cell development in the convergent Cascadia margin

- of the Pacific Northwest, USA. In: Osborne, R. (Ed.), *From Shoreline to the Abyss, Contributions in Marine Geology in Honor of F.P. Shepard*, SEPM Special Publication, vol. 46, pp. 17–34.
- Peterson, C., Baham, J., Beckstrand, D., Clough, C., Cloyd, C., Erlandson, J., Grathoff, G., Hart, R., Jol, H., Percy, D., Reckendorf, F., Rosenfeld, C., Smith, T., Phyllis Steeves, P., Stock, E., 2002. Field guide to the Pleistocene and Holocene dunal landscapes of the Central Oregon Coast: Newport to Florence, Oregon. Geological Society of America, Field Trips Guide, Cordillera Meeting, Corvallis, Oregon. 13 pp.
- Peterson, C., Stock, E., Cloyd, C., Beckstrand, D., Clough, C., Erlandson, J., Hart, R., Murillo-Jiménez, Percy, D., Price, D., Reckendorf, F., Vanderburgh, S., 2006. Dating and morphostratigraphy of coastal dune sheets from the central west coast of North America. Oregon Sea Grant Publications, Corvallis, Oregon. 95 pp.
- Pirazzoli, P.A., 1993. Global sea-level changes and their measurement. *Global and Planetary Change* 8, 135–148.
- Rankin, D.K., 1983. Holocene geologic history of the Clatsop plains foredune ridge complex: M.S. Thesis. Portland State University, Portland, Oregon, 175 p.
- Reckendorf, F., 1975. Beaches and dunes of the Oregon coast. US Department of Agriculture, Oregon Department of Soil Conservation Service, and Oregon Coastal Conservation and Development Commission. 161 pp.
- Reckendorf, F., 1998. Geologic hazards of development on sand dunes along the Oregon coast. In: Burns, S. (Ed.), *Environmental, Groundwater, and Engineering Geology: Applications from Oregon*. Star Publishing Company, Belmont, CA, pp. 429–438.
- Reckendorf, F., Peterson, C., Percy, D., 2001. Dune ridges of Clatsop County. Department of Oregon Geology and Mineral Industries, Open-File Report 0–01–07, Text and Interactive Map on CDROM.
- Reneau, S.L., Dietrich, W.E., Dom, R.I., Berger, C.R., Rubin, M., 1986. Geomorphic and paleoclimatic implications of latest Pleistocene radiocarbon dates from colluvium-mantled hollows, California. *Geology* 14, 655–658.
- Rypins, S., Reneau, S.L., Byrne, R., Montgomery, D.R., 1989. Palynologic and geomorphic evidence for environmental change during the Pleistocene–Holocene transition at Point Reyes Peninsula, central coastal California. *Quaternary Research* 32, 72–87.
- Schiedegger, K.F., Kulm, L.D., Runge, E.J., 1971. Sediment sources and dispersal patterns of Oregon continental shelf sands. *Journal of Sedimentary Petrology* 41, 1112–1120.
- Schlicker, H.G., Deacon, R.J., 1974. Environmental Geology of Lane County Oregon. Oregon Department of Geology and mineral Industries, Bulletin, vol. 85. 116 pp.
- Schlicker, H.G., Deacon, R.J., Olcott, G.W.M., Beaulieu, J.D., 1973. Environmental Geology of Lincoln County Oregon. Oregon Department of Geology and mineral Industries, Bulletin, vol. 81. 171 pp.
- Shultz, S.T., 1998. Dunes and Freshwater Wetlands. The Northwest Coast, a Natural History. Timber Press, Portland, Oregon, pp. 223–253.
- Stuiver, M., Reimer, P.J., Braziunas, T.F., 1998. High-precision radiocarbon age calibration for terrestrial and marine samples. *Radiocarbon* 40, 1127–1151.
- Tasa, G.L., Connolly, T.J., 1995. Archaeological evaluation of the Boiler Bay site (35LNC45). In the Boiler Bay State Park Section of the Oregon Coast Highway (US 101), Lincoln County, Oregon, OSMA Report 95–1, State Museum of Anthropology, University of Oregon.
- Tveskov, M.A., Erlandson, J.M., Moss, M.L., 1996. Archaeological investigations at the Coquille Point Site (35CS136), Coos County, Oregon. Report of the Coastal Prehistory Program, Department of Anthropology and State Museum of Anthropology, University of Oregon.
- United States Forest Service, 1994. Management plan for the Oregon Dunes National Recreation Area, Siuslaw National Forest, Coos, Douglas, and Lane counties. U.S. Dept. of Agriculture, Forest Service, Pacific Northwest Region.
- Wiedemann, A.M., 1990. The coastal parabolic dune system at Sand Lake, Tillamook County, Oregon, USA. In: Davidson-Arnott, R. (Ed.), *Proceedings of the Symposium on Coastal Sand Dunes 1990*. National Research Council, Ottawa, pp. 341–358.
- Worona, M.A., Whitlock, C., 1995. Late Quaternary vegetation and climate history near Little Lake, central Coast Range, Oregon. *Geological Society America Bulletin* 107, 867–876.
- Woxell, L.K., 1998. Prehistoric beach accretion rates and long-term response to sediment depletion in the Columbia River littoral system, USA: M.S. Thesis, Portland State University, Portland, Oregon, 206 p.